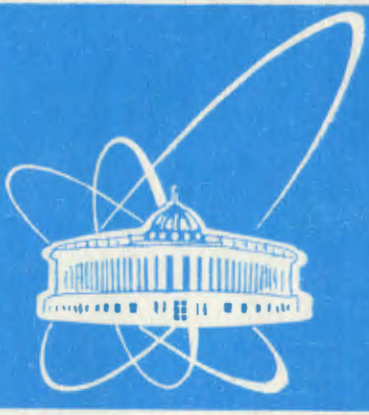

объединенный
институт
ядерных
исследований
дубна

E2-94-353

S.G.Mashnik, S.A.Smolyansky[1]

THE CASCADE-EXCITON APPROACH TO NUCLEAR REACTIONS

(Foundation and Achievements)

A short version of the invited lectures given at the International Study Centre in Nonlinear Science «Dynamics of Transport in Fluid, Plasmas and Charged Beams», Villa Gualino, Torino, Italy, June—September, 1994

[1]Physics Department, Saratov State University, 410071 Saratov, Russia

1994

1. Introduction

A large amount of nuclear reaction data at medium energies is required for different important applications, e.g., for recent plans of transmutation of long-lived radioactive wastes with a spallation source, medical and biomedical needs, and research of cosmic-ray effects on spaceships and astronauts. Experiments to measure these data are costly and there are a limited number of facilities available to make these measurements. Therefore reliable models are required to provide the necessary data.

On the other hand, for solving different purely academic problems, such as investigations of quark and gluon degrees of freedom of nuclei, medium effect on structure of hadrons and their interactions, mechanisms of cumulative and subthreshold particle production, one needs to estimate the role of common "background" nuclear effects, again using reliable models. One model like that may be our Cascade-Exciton Model (CEM) of nuclear reactions[1], initially proposed to describe nucleon-induced reactions at bombarding energies below or at $\sim$ 100 MeV and developed after that for a larger interval of incident nucleon and pion bombarding energies (see, e.g., Refs.[2, 3] and references given therein), for the description of stopped negative pion absorption by nuclei (see Ref.[4] and references given therein), and for the description of photonuclear reactions[5].

The aim of the present lectures is to obtain and analyze the relativistic kinetic equations describing different stages of nuclear reactions in the CEM, to show the main assumptions of our model and to demonstrate exemplary results obtained in the framework of the CEM.

2. Foundation of the CEM Basic Equations

We are going to obtain here kinetic equations (KE) for nucleon-antinucleon medium taking into account such relativistic effects as delay of interaction, particle-antiparticle states, spin of the constituents, meson degrees of freedom, etc. For this aim we use the Zubarev method of the non-equilibrium statistical operator. This method occupies a special place as compared to the well known BBGKI[6, 7] and the contour Green functions[8]-[12] approaches, as it allows to derive generalized KE in a very general form without detailing specific properties of a system. This is especially important for treating complex systems with many degrees of freedom.

In the relativistic region, the Zubarev method was realized at the kinetic stage of a system evolution in Ref.[13]. The generalized relativistic KE were obtained in terms of the relativistic Wigner functions

$$\begin{aligned} f_{\alpha\beta}(x,p) &= (2\pi)^{-4}\int dy e^{-ipy} < P_{\alpha\beta}(x,y) >_\tau = \\ &= (2\pi)^{-4}\int dy e^{-ipy} < \bar{\Psi}_\beta(x+\frac{y}{2})\Psi_\alpha(x-\frac{y}{2}) >_\tau . \end{aligned} \qquad (1)$$

Here, the Greek indices denote the sort, polarization and other characteristics of particles, x is the 4-vector of the Minkowski space, and p is the 4-vector of momentum space. For generality, the statistics of the fields $\bar{\Psi}_\beta, \Psi_\alpha$ is not fixed here. The main difference of this definition from the standard one consists in an averaging procedure which should be done by means of the non-equilibrium statistical operator $\rho(\tau)$, i.e., $< ... >_\tau = Sp...\rho(\tau)$. Let us define the "proper time" τ. For this, one introduces the atlas of maps. Each map consists

of congruence space-like hyperplanes $\sigma(n,\tau)$ whose orientation in the Minkowski space is determined by a unit time-like vector directed towards the future:

$$n^\mu = p^\mu/\sqrt{p^2} = u^\mu\ , \qquad p^2 \geq 0\ . \tag{2}$$

So, we have $\tau = xu$. The family of hyperplanes is parametrized by τ; and the maps from atlas, by the normal vector u^μ (the 4-velocity of the "tasted particle").

Now we can introduce the quantum relativistic Liouville equation for the non-equilibrium statistical operator (the interaction picture)

$$\frac{\partial\rho}{\partial\tau} - i[\rho(\tau), H_{int}(\tau)] = -\epsilon\{\rho(\tau) - \rho_q(\tau)\}\ , \qquad \epsilon > 0\ . \tag{3}$$

This equation has an infinitly small source in its right-hand side which allows one to select out retarded solutions of the Liouville equation in full analogy with the formal scattering theory. The source intensity is governed by the parameter $\epsilon > 0$. It implies that after fulfilling a calculation, the thermodynamical limit should be taken and then $\epsilon \to 0$. The quasi-equilibrium statistical operator $\rho_q(\tau)$ is an asymptotic form of the non-equilibrium operator $\rho(\tau)$ at the kinetic stage of evolution. An explicit form of the operator $\rho_q(\tau)$ is found from extremum of the information entropy functional of the quasi-equilibrium state

$$< S(\tau) >_{q\tau} = - < ln\rho_q(\tau) >_{q\tau} = -Sp\ \rho_q(\tau) ln\rho_q(\tau) \tag{4}$$

at a given averaged value of $< P(x,y) >_{q\tau}$ and a normalization condition $< 1 >_{q\tau} = 1$. It results in the following structure of the quasi-equilibrium statistical operator

$$\rho_q(\tau) = exp\{-S(\tau)\}\ , \tag{5}$$

where $S(\tau)$ is the entropy operator at the kinetic stage

$$S(\tau) = \Phi(\tau) + \int d\sigma(x \mid u) \int d^4y P_{\alpha\beta}(x,y) F_{\alpha\beta}(x,y)\ . \tag{6}$$

Here, the function $F_{\alpha\beta}(x,y)$ is the Lagrange factor corresponding to $< P_{\alpha\beta}(x,y) >_{q\tau}$ and $\Phi(\tau)$ is a normalizing functional providing the condition $< 1 >_{q\tau} = 1$. The operator structure of $\rho(\tau)$ allows us to take advantage of the Wick-Bloch-Donincis theorem and to derive a closed KE.

It is very important that at the kinetic stage of evolution, the statistical operators $\rho(\tau)$ and $\rho_q(\tau)$ are completely equivalent in the sense that $< P(x,y) >_\tau = < P(x,y) >_{q\tau}$ (the self-consistency condition).

Now we can construct different approximately truncated schemes. We use the perturbation theory with the small parameter *(Anzatz I)*

$$|< H_{int} > / < H_0 >| \ll 1\ . \tag{7}$$

As a rule, this condition is correct in nuclear physics at intermediate energies. The following generalized KE is derived for this case:

$$p\frac{\partial f(x,p)}{\partial x} = I^{(1)}(x,p) + I^{(2)}(x,p) \tag{8}$$

with CI of the first and second orders

$$I^{(1)}_{\alpha\beta}(x,y) = -i\sqrt{p^2}(2\pi)^{-4}\int dy e^{-ipy} < [P_{\alpha\beta}(x,y), H_{int}(\tau)] >_{q\tau} ,$$

$$I^{(2)}_{\alpha\beta}(x,y) = -\sqrt{p^2}(2\pi)^{-4}\int dy e^{-ipy}\int\limits_{-\infty}^{\tau} d\tau' e^{\epsilon(\tau'-\tau)} \times$$

$$\times < [H_{int}(\tau'), [H_{int}(\tau), P_{\alpha\beta}(x,y)]] >_{q\tau'} + I^{\prime(2)}_{\alpha\beta}(x,p) , \qquad (9)$$

where $I^{\prime(2)}_{\alpha\beta}(x,p)$ is a compensational function. Further analysis of these CI is possible only upon specifying the system of interacting fields.

Many results on this CI have been obtained by now in literature for different versions of the Walecka relativistic nuclear models. Let us regard here two types of vertices: "three-legged" (barion-barion-meson) and "four-legged" (baryon-barion) (see Fig. 1).

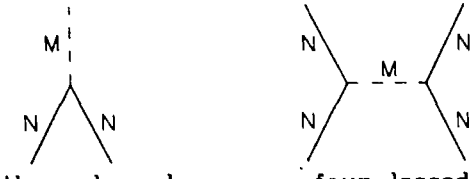

Fig. 1

The results obtained by different authors for the Walecka models are summarized in Table 1. In order to ground the CEM and to have a possibility of its generalization, let us write CI of the Relativistic Boltzmann-Uehling-Uhlenbeck (RBUU) type in the nuclear sector of the Walecka model with vertices of the "four-legged" type with the Hamiltonian density *(Anzatz II)*

$$H_{int}(x) = \int dx' \Psi_1(x)\Psi_{1'}(x')V_{11',22'}(x-x')\Psi_{2'}(x)\Psi_2(x) . \qquad (10)$$

Then, we can get CI of the RBUU type with a full set of relativistic effects and with virtual meson degrees of freedom, which defines the quasipotential $V_{11',22'}(x)$ of the system [15]:

$$I^{(2)}_{\alpha\beta}(x,p) = -\int\prod_1^4 dp_i \omega_{\alpha\beta;11',22',33',44'}(p \mid p_1,p_2,p_3,p_4) \times$$

$$\times \{f_{11'}(x,p_1)f_{22'}(x,p_2)f_{33'}(x,p_3)f_{44'}(x,p_4) -$$

$$- f_{11'}(x,p_1)f_{22'}(x,p_2)f_{33'}(x,p_3)f_{44'}(x,p_4)\} . \qquad (11)$$

Let us define the notation. The numerical indices correspond to the spin degrees of freedom. The relativistic Pauli blocking factor is defined in the following way:

$$f_{11'}(x,p) = \frac{1}{\hat{\gamma}}(2\pi)^4 S_{11'}(-p) - f_{11'}(x,p) , \qquad (12)$$

where $S_{11'}(p)$ is the Fourier transform of the fermionic commutative function

$$[\Psi_\alpha(x), \Psi_\beta(y)]_+ = -iS_{\alpha\beta}(x-y) . \qquad (13)$$

Table 1

The first order, $I^{(1)}_{\alpha\beta}(x,p)$					
KE of the Vlasov type ("Tree-legged" vertices)			KE of Vlasov type ("Four-legged" vertices)		
N sector	Δ sector	meson sector	N sector	Δ sector	meson sector
[8], [9], [16]-[20]	–	is absent	–	[14]	is absent
The second order, $I^{(2)}_{\alpha\beta}(x,p)$					
KE of the Bloch type ("Tree-legged" vertices)			KE of Boltzmann type ("Four-legged" vertices)		
N sector	Δ sector	meson sector	N sector	Δ sector	meson sector
[13]	–	[13]	[15], [9]-[12]	–	is absent

In comparison with the usual Boltzmann CI, our CI (11) has a more complicated structure because the corresponding transition matrix has a non-diagonal form

$$\begin{aligned}
&\omega_{\alpha\beta;1'1',2'2',3'3',4'4'}(p \mid p_1,p_2,p_3,p_4) = \\
&= (2\pi)^8\delta(p_1+p_2-p_3-p_4)\delta(p-p_1)\times \\
&\times \{\delta_{\alpha 1'}V'_{\beta 2',43}(p_1-p_4)[\tilde{V}_{4'3',21}(p_1-p_3)-\tilde{V}_{3'4',21}(p_1-p_4)]+ \\
&+ \delta_{\beta 1}V''_{3'4',\alpha 2}(p_1-p_3)[\tilde{V}_{1'2',34}(p_1-p_3)-\tilde{V}_{1'2',43}(p_1-p_4)]\}
\end{aligned} \tag{14}$$

with

$$\begin{aligned}
V'_{\beta 1',22'}(p-p_1) &= \hat{\gamma}_{\beta 1}V_{11',22'}(p_1-p)+ \\
&+ \frac{1}{i}\int d\omega V_{11',22'}(p-p_1+\omega u)S_{\beta 1}(p+\omega u)\,, \\
V''_{11',\alpha 2'}(p-p_1) &= \hat{\gamma}_{2\alpha}V_{11',22'}(p-p_1)+ \\
&+ \frac{1}{i}\int d\omega V_{11',22'}(p_1-p+\omega u)S_{2\alpha}(p-\omega u)\,.
\end{aligned} \tag{15}$$

Here $V_{11',22'}(p)$ is the Fourier transform of the quasipotential $V_{11',22'}(x)$ and $\hat{\gamma}_{11'}=p\gamma_{11'}$. At last, we have

$$\tilde{V}_{11',22'}(x)=\frac{1}{2}\{V_{11',22'}(x)+V_{1'1,2'2}(-x)\}\,. \tag{16}$$

In CI (11) we neglect the deviation of the system's behavior from the Markovian one, and assume that all Wigner functions in (11) can be considered in one space-time dot *(Anzatz III)*.

CI (11) corresponds to connected self-energetical diagrams only. We neglect diagrams of the "tadpole" type which lead to the renormalizations of interaction *(Anzatz IV)*. All the other relativistic effects are taken into account exactly.

Let us see now how we can obtain the usual Boltzmann-Uehling-Uhlenbeck (BUU) KE. The relativistic Wigner function includes the states with both positive and negative energies. So, CI (11) contains really two KE for particles and antiparticles. We can assume now that the role of antibaryons is small and can be neglected *(Anzatz V)*.

Let us note that the nucleons of the nuclear matter are not free. Generally, they have effective masses M_N^* which differ from ones at the free stage (m_N): $M_N^* \neq m_N$. Let us state that the Wigner function of the stages with positive energies do not contain the assumption that baryons are on the mass-shell. This is important in some cases. For example, the Δ-isobar has the distributed mass. Now, for simplicity, let us assume that for nucleons of the system the on-mass-shell condition is satisfied, i.e.,$p^0 = \sqrt{M_N^{*2} + \vec{p}^2}$ *(Anzatz VI)*. Simultaneously we pass from the spinor representation of the Wigner functions to the spin one

$$f_{\alpha\beta}^{(+)}(x,p) = F_{rs}(x,\vec{p}) u_\alpha^r(p) \bar{u}_\beta^s(p) \delta(p^2 - M_N^{*}) \epsilon(p^0) , \qquad (r,s = 1,2) . \qquad (17)$$

Here $u_\alpha^r(p)$ is the free spinor which satisfies the free Dirac equation with the mass M_N^*.

Now we take away one more relativistic effect, namely, the delay of a nucleon-nucleon interaction *(Anzatz VII)*. Then, the quasipotential passes to the nuclear potential, $V_{11',22'}(p) \Rightarrow \delta(p^0) V_{11',22'}(\vec{p})$. This procedure leads to a considerable simplification of CI (11). As a result, we obtain the quantum CI of the Kadanoff-Beym type. It takes into account only the relativistic spin and kinematical effects.

The next simplification is connected with neglecting the spin effects *(Anzatz VIII)*. It leads to the quantum BUU-type KE with relativistic kinematical effects only.

In a classical limit *(Anzatz IX)*, we get the relativistic Boltzmann KE which we write by using the differential cross section

$$\frac{\partial f_k}{\partial t} + \vec{v}\frac{\partial f_k}{\partial \vec{x}} + \vec{F}\frac{\partial f_k}{\partial \vec{p}} = \int\int d^3p_l d\Omega v_{rel} \frac{d\sigma(v_{rel})}{d\Omega} (f_i f_j - f_k f_l) . \qquad (18)$$

Here $\vec{F}$ is a force corresponding to the self-consistent nuclear field (see Table 1).

Up to now, we have considered nuclear matter in the thermodynamical limit ($V \to \infty$, $N \to \infty$, $n = N/V = const$). We can introduce now a final volume V of the system and a set of parameters for the inner degrees of freedom *(Anzatz X)*. This step can be done in a phenomenological way only. It is equivalent to the transition to an open system and leads at once to the following BUU KE:

$$\begin{aligned} \frac{\partial f_k}{\partial t} + \vec{v}\frac{\partial f_k}{\partial \vec{x}} + \vec{F}\frac{\partial f_k}{\partial \vec{p}} &= \sum_{ijl} \{ A_{ij\to kl} f_i f_j [1+f_k][1+f_l] - \\ &- A_{kl\to ij} f_k f_l [1+f_i][1+f_j] \} . \end{aligned} \qquad (19)$$

The Boltzmann KE (18) is the base for the description of fast processes in the intranuclear cascade models. In these models, the fast (cascade) particles and the target-nucleus nucleons, which nave not yet been involved in the interaction, are considered as two different types of particles, and the collisions between particles of the same type are neglected. The nuclear constituents are believed to be described by the equilibrium (maxwellian) distribution function $f^T(\vec{r},\vec{p})$. Then, for the distribution function of cascade particles $f^{cas}(\vec{r},\vec{p},t)$ from Eq. (18) we have (in the linear approximation):

$$\left(\frac{\partial}{\partial t} + \frac{\vec{p}}{m}\cdot\vec{\nabla}_{\vec{r}} + \vec{F}\cdot\vec{\nabla}_{\vec{p}}\right) f^{cas}(\vec{r},\vec{p},t) = -\rho^T(\vec{r}) < \sigma v_{rel} > f^{cas}(\vec{r},\vec{p},t) + Q(\vec{r},\vec{p},t) . \qquad (20)$$

According to the normalization of the single-particle distribution function,

$$\rho^T(\vec{r}) = \int d\vec{p} f^T(\vec{r},\vec{p}) \tag{21}$$

is the local particle number density. Averaging in (20) is carried over the distribution function of the target nucleus nucleons

$$< \sigma v_{rel} >= \frac{1}{\rho^T(\vec{r})} \int d\vec{p} f^T(\vec{r},\vec{p}) \sigma(v_{rel}) v_{rel} \ , \tag{22}$$

and the cross section $\sigma(v_{rel})$ allows for the exclusion principle. The source function in the right-hand side of (20) is

$$Q(r,p,t) = \int\int d\vec{p}_i d\Omega v_{rel} \frac{d\sigma(v_{rel})}{d\Omega} f^T(\vec{r},\vec{p}_i) f^{cas}(\vec{r},\vec{p}_j,t) \ . \tag{23}$$

The integro-differential equation (20) can be transformed into the integral one. In particular, if the fast particle flux collides with the semi-infinite slab of nuclear matter, we have for the cascade particles (neglecting recoil nucleons and assuming for simplicity $\rho^T = const$ and $\vec{F} = 0$)

$$\begin{aligned} f^{cas}(\vec{r},\vec{p},t) &= N_0 \delta(\vec{p}-\vec{p}_0) exp\left[-\int_0^t dt' \rho^T < \sigma v_{rel} >\right] + \\ &+ \int_0^t dt'' \rho^T \rho^{cas}\left(\vec{r} - \frac{\vec{p}}{m}(t-t''), t''\right) Q\left(\vec{r} - \frac{\vec{p}}{m}(t-t''), \vec{p}, t''\right) \times \\ &\times \ exp\left[-\int_{t''}^t dt' \rho^T < \sigma v_{rel} >\right] \ , \end{aligned} \tag{24}$$

where $\rho^{cas}(\vec{r},t)$ is related to $f^{cas}(\vec{r},\vec{p},t)$ by an equation of the type (21). The probabilistic interpretation of this equation is quite obvious: A number of particles at the given point $\vec{r}$ having momentum within the interval $d\vec{p}$ around the value $\vec{p}$ is built of the incident beam N_0 reaching this point (with an exponential damped factor) and rescatterings of every kind resulting in particles of interest. Relation (24) and its probabilistic interpretation are grounds for the cascade model proceeding from an analogy between the interaction of fast particles with nuclei and high-energy radiation transport through matter[21]. In a real case, one needs to solve the related system of integral equations like (24) with a distributed source function and complex initial and boundary conditions. It turns out to be more effective to use the analogy mentioned above and on this basis to simulate the fate of every particle inside a nucleus by the Monte Carlo technique.

As it has been shown in Ref.[1], the KE (19) can be rewritten in a form of the master equation

$$\frac{\partial P(E,\alpha,t)}{\partial t} = \sum_{\alpha \neq \alpha'} [\lambda(E\alpha, E\alpha') P(E,\alpha',t) - \lambda(E\alpha', E\alpha) P(E,\alpha,t)] \ . \tag{25}$$

Here $P(E,\alpha,t)$ is the probability of finding the system at the time moment t in the $E\alpha$ state, and $\lambda(E\alpha,E\alpha')$ is the energy-conserving probability rate, defined in the first order of the time-depending perturbation theory,

$$\lambda(E\alpha,E\alpha') = \frac{2\pi}{\hbar}|<E\alpha|\hat{V}|E\alpha'>|^2\omega_\alpha(E)\ . \qquad (26)$$

The matrix element $<E\alpha|\hat{V}|E\alpha'>$ is believed to be a smooth function in energy, and $\omega_\alpha(E)$ is the density of the final state of the system. One should note that Eq. (25) is derived provided that the "memory" time τ_{mem} of the system is small compared to the characteristic time for intranuclear transition $\sim \hbar/\lambda(E\alpha,E\alpha')$ but, on the other hand, Eq. (25) itself is applicable for the time moments $t \gg \hbar/\lambda(E\alpha,E\alpha')$. Due to the condition $\tau_{mem} \gg \hbar/\lambda(E\alpha,E\alpha')$, being describing by Eq. (25), the random process is the markovian one.

The master equation (25) is usually used to describe the relaxation phenomena at the pre-equilibrium stage of nuclear reactions in the framework of the so called exciton models. Within these models, an excited nuclear state is completely defined by an excitation energy and a number of excited particles p and holes h ($n = p + h$ is a number of excitons), that is $\alpha \equiv n$. A further simplification is achieved by assuming that the sum $\sum_{\alpha'\neq\alpha}$ in the right-hand side of (25) is contributed only by the terms representing the exciton-exciton scattering, that gives rise to the selection rule $\Delta n = 0,\ \pm 2$ under intranuclear transitions.

So, we have shown that it is possible to pass from KE (11) to (24) and (25) by means of several anzatzes. The decline of some concrete anzatzes will arise the corresponding generalizations of the simplest KE (24) and (25).

3. Basic Assumptions of the CEM

A detailed description of the CEM may be found in Ref.[1], therefore, only its basic assumptions will be outlined here. The physical picture underlying our model is rather natural. A particle entering a nucleus can suffer one or several intranuclear collisions, that gives rise to the formation of an excited many-quasiparticle state like a "doorway state". Due to residual interaction this state will evolve towards a more complicated one up to the formation of a compound nucleus. At each stage of this process a particle can be emitted. The behaviour of a primary particle and of those of second and subsequent generations (if any) up to their capture or emergence from a nucleus is treated in the framework of the intranuclear cascade model. The number of captured nucleons and "holes" produced due to the intranuclear collisions gives us the initial particle-hole configuration of the remaining excited nucleus, the excitation energy of which is defined by the conservation laws. A further destiny of the nucleus is traced in terms of the exciton model of pre-equilibrium decay which includes in a natural way the particle decay at the equilibrium stage too.

Thus, the CEM considers the nuclear reaction as proceeding through three stages – cascade, pre-equilibrium and equilibrium (or compound nucleus). So, in a general case, the three components may contribute to any experimentally measured quantity. In particular, for the inclusive particle spectrum to be discussed later, we have

$$\sigma(\vec{p})d\vec{p} = \sigma_{in}[N^{cas}(\vec{p}) + N^{pre}(\vec{p}) + N^{eq}(\vec{p})]d\vec{p}\ . \qquad (27)$$

The cascade stage of the interaction is described by the Dubna version of the intranuclear cascade model (ICM)[21]. The Monte Carlo solution of the system of integral equations

like (24) gives the single-particle distribution function $f^{cas}(\vec{r},\vec{p},t)$ through which all needed characteristics can be expressed. For example, for $N^{cas}(\vec{p})$ from (27) we have

$$N^{cas}(\vec{p})d\vec{p} = \frac{1}{\sigma_{in}} \int_0^R d^2b \int_{r>R} d\vec{r} \int_0^{t_{cas}} dt f_b^{cas}(\vec{r},\vec{p},t)d\vec{p}\,, \tag{28}$$

where the integration is carried out over all accessible impact parameters b for particles leaving a nucleus of radius R by the end of the cascade stage t_{cas}. It is noteworthy that, being defined by the size of the nucleus and its transparency (see the first term in equation (24)), the reaction cross section σ_{in} is calculated within the cascade model itself. Hence, the CEM predicts the absolute values for calculated characteristics and does not require any additional data or special normalization of its results.

All the cascade calculations are carried out in a three-dimensional geometry. The nuclear matter density $\rho^T(r)$ is described by the Fermi distribution with two parameters taken from the analysis of electron-nucleus scattering. Practically, the nucleus target is divided by concentric spheres into seven zones in which the nuclear density is considered to be constant. The energy spectrum of nuclear nucleons is estimated in the perfect Fermi gas approximation with the local Fermi energy $T_F(r) = \hbar^2[3\pi^2\rho^T(r)]^{2/3}/(2m_N)$, where m_N is the nucleon mass. The influence of intranuclear nucleons on the incoming projectile is taken into account by adding to its laboratory kinetic energy an effective real potential V, as well as by taking into account the Pauli principle which forbids a number of intranuclear collisions and effectively increases the mean path free of fast particles inside the target. For incident nucleons $V \equiv V_N(r) = T_F(r)+\epsilon$, where $T_F(r)$ is the corresponding Fermi energy and ϵ is the mean binding energy of the nucleons ($\epsilon \simeq 7$ MeV [21]). For pions, in the Dubna ICM usually one uses [21] a square-well potential with the depth $V_\pi \simeq 25$ MeV, independently of the nucleus and pion energy. The interaction of the incident particle with the nucleus comes to a series of successive quasifree collisions of the fast cascade particles (π or N) with intranuclear nucleons:

$$\begin{aligned} NN \to NN, \qquad NN \to \pi NN, \qquad NN \to \pi_1,\cdots,\pi_i NN \\ \pi N \to \pi N, \qquad \pi N \to \pi_1,\cdots,\pi_i N \qquad (i \geq 2)\,. \end{aligned} \tag{29}$$

To describe these elementary collisions, one uses the experimental cross sections for the free πN and NN interactions approximated by special polynomial expressions with energy-dependent coefficients [21] and one takes into account the Pauli principle.

The Pauli exclusion principle at the cascade stage of the reaction is handled in the following way: one assumes that nucleons of the target occupy all the energy levels up to the Fermi energy. Each simulated elastic or inelastic interaction of the projectile (or of a cascade particle) with a nucleon of the target is considered forbidden if the "secondary" nucleons have energies smaller than the Fermi energy. If so, the trajectory of the particle is traced further from the forbidden point and a new interaction point, a new partner and a new interaction mode are simulated for the traced particle, and so on, until the Pauli principle is kept or the particle leaves the nucleus.

Besides the elementary processes (1), the Dubna ICM takes also into account pion absorption on the nuclear pairs

$$\pi NN \to NN\,. \tag{30}$$

The momenta of two nucleons participating in the absorption are chosen randomly from the Fermi distribution, and the pion energy is distributed equally between these nucleons in the center-of-mass system of the pion and nucleons participating in the absorption. The direction of motion of the resultant nucleons in this system is taken as isotropically distributed in space. The effective cross section for absorption is estimated from the experimental cross-section of pion absorption by deuterons. The Dubna ICM is described in detail in the monograph [21].

The subsequent interaction stages are considered in the framework of the modified exciton model[22]. The model uses effectively the relationship of the master equation (25) with the markovian random processes. Indeed, an attainment of the statistical equilibration described by Eq. (25) is an example of the discontinuous markovian process: The temporal variable changes continuously and at a random moment the state of the system changes by a discontinuous jump, the behaviour of the system at the next moment being completely defined by its state at present. As long as the transition probabilities $\lambda(E\alpha, E\alpha')$ are time independent, the waiting time for the system in the $E\alpha$ state has the exponential distribution (the Poisson flow) with the average lifetime $\hbar/\Lambda(\alpha, E) = \hbar/\sum_{\alpha'} \lambda(E\alpha, E\alpha')$. This fact prompts a simple method of solving the related system of Eq. (25): Simulation of the random process by the Monte Carlo technique. In this treatment it is possible to generalize the exciton model to all nuclear transitions with $\Delta n = 0, \pm 2$, and the multiple emission of particles and to depletion of nuclear states due to the particle emission. In this case the system (25) is as follows:

$$\begin{aligned}\frac{\partial P(E,\alpha,t)}{\partial t} &= -\Lambda(n,E)P(E,n,t) + \lambda_+(n-2,E)P(E,n-2,t) + \\ &+ \lambda_0(n,E)P(E,n,t) + \lambda_-(n+2,E)P(E,n+2,t) + \\ &+ \sum_j \int dT \int dE' \lambda_c^j(n,E,T)P(E',n+n_j,t)\delta(E'-E-B_j-T) \quad (31)\end{aligned}$$

The lifetime of the excited system at the state with $n = p + h$ excitons (but with different p-, h-composition (for details see Ref.[1]) is given by

$$\frac{\hbar}{\Lambda(n,E)} \equiv \frac{\hbar}{\Lambda(p,h,E)} = \hbar[\lambda_+(p,h,E)+\lambda_0(p,h,E)+\lambda_-(p,h,E)+\sum_j \Gamma_j(p,h,E)]^{-1} , \quad (32)$$

where according to (26) the partial transition probabilities changing the exciton number by Δn are

$$\lambda_{\Delta n}(p,h,E) = \frac{2\pi}{\hbar}|M_{\Delta n}|^2 \omega_{\Delta n}(p,h,E) , \quad (33)$$

and the emission rate of a nucleon of the type j into the continuum is estimated according to the detailed balance principle

$$\begin{aligned}\Gamma_j(p,h,E) &= \int_{V_j^c}^{E-B_j} \lambda_c^j(p,h,E,T)dT , \\ \lambda_c^j(p,h,E,T) &= \frac{2s_j+1}{\pi^2\hbar^3}\mu_j \Re_j(p,h)\frac{\omega(p-1,h,E-B_j-T)}{\omega(p,h,E)}T\sigma_{inv}(T) , \quad (34)\end{aligned}$$

where s_j, B_j, V_j^c, and μ_j are the spin, binding energy, Coulomb barrier, and reduced mass of the emitted particle, respectively. A modification of (34) for the complex particle emission is

discussed in detail in Ref.[1]. The factor $\Re_j(p,h)$ ensures the condition for the exciton chosen to be the nucleon of type j. This factor can easily be calculated by the Monte Carlo technique.

Assuming an equidistant level scheme with the single-particle density g, we have the level density of the n-exciton state as[23]

$$\omega(p,h,E) = \frac{g(gE)^{p+h-1}}{p!h!(p+h-1)!} \,. \tag{35}$$

This expression should be substituted into Eq. (34). For the transition rates (33), one needs the number of states by taking into account the selection rules for intranuclear exciton-exciton scattering. The appropriate formulae have been derived by Williams[24] and later corrected for the exclusion principle and indistinguishability of identical excitons in Ref.[25]:

$$\begin{aligned}
\omega_+(p,h,E) &= \frac{1}{2}g\frac{[gE-\mathcal{A}(p+1,h+1)]^2}{n+1}\left[\frac{gE-\mathcal{A}(p+1,h+1)}{gE-\mathcal{A}(p,h)}\right]^{n-1} , \\
\omega_0(p,h,E) &= \frac{1}{2}g\frac{[gE-\mathcal{A}(p,h)]}{n}[p(p-1)+4ph+h(h-1)] , \\
\omega_-(p,h,E) &= \frac{1}{2}gph(n-2) \,,
\end{aligned} \tag{36}$$

where $\mathcal{A}(p,h) = (p^2+h^2+p-h)/4 - h/2$. By neglecting the difference of matrix elements with different Δn, $M_+ = M_- = M_0 = M$, we estimate the value of M for a given nuclear state by association of the $\lambda_+(p,h,E)$ transition with the probability for quasi-free scattering of a nucleon, which is above the Fermi level, on a nucleon of the target nucleus. Therefore, we have

$$\frac{<\sigma(v_{rel})v_{rel}>}{V_{int}} = \frac{\pi}{\hbar}|M|^2\frac{g[gE-\mathcal{A}(p+1,h+1)]}{n+1}\left[\frac{gE-\mathcal{A}(p+1,h+1)}{gE-\mathcal{A}(p,h)}\right]^{n-1} , \tag{37}$$

where V_{int} is the interaction volume, and the averaging in the left-hand side of (37) is carried out over all excited states taking into account the exclusion principle. Combining (33), (35) and (37), we get finally for the transition rates:

$$\begin{aligned}
\lambda_+(p,h,E) &= \frac{<\sigma(v_{rel})v_{rel}>}{V_{int}} \,, \\
\lambda_0(p,h,E) &= \frac{<\sigma(v_{rel})v_{rel}>}{V_{int}}\frac{n+1}{n}\left[\frac{gE-\mathcal{A}(p,h)}{gE-\mathcal{A}(p+1,h+1)}\right]^{n+1}\frac{p(p-1)+4ph+h(h-1)}{gE-\mathcal{A}(p,h)} , \\
\lambda_-(p,h,E) &= \frac{<\sigma(v_{rel})v_{rel}>}{V_{int}}\left[\frac{gE-\mathcal{A}(p,h)}{gE-\mathcal{A}(p+1,h+1)}\right]^{n+1}\frac{ph(n+1)(n-2)}{[gE-\mathcal{A}(p,h)]^2} \,.
\end{aligned} \tag{38}$$

Thus, the initial conditions for the system of Eqs. (31), $t_0 = t_{cas}$, n_0, E_0, are calculated within the cascade model. The Monte Carlo solution of (31) gives the population probabilities for the n-exciton states $P(E,n,t)$. By the pre-equilibrium particles we call those which have been emitted before achieving of the statistical equilibrium appropriating to the time moment t_{eq}. This moment is fixed by the condition $\lambda_+(n_{eq},E) = \lambda_-(n_{eq},E)$ from which we get

$n_{eq} \simeq \sqrt{2gE}$. The pre-equilibrium component in (27) for the inclusive spectrum of particles of the type j can be represented as

$$N^{pre}(\vec{p})d\vec{p} = \int_{t_{cas}}^{t_{eq}} dt \sum_n \lambda_j^i(n,E,T)P(E,n,t)\frac{\partial(p,\Omega)}{\partial(T,\Omega)}F(\Omega)dTd\Omega \ . \qquad (39)$$

We shall return to the discussion of the angular anisotropy later. Here, we note only that the angular function $F(\Omega)$ is normalized to unity, $\int d\Omega F(\Omega) = 1$.

Similarly to (39) we can write down the expression for the equilibrium ($n \geq n_{eq}$) component:

$$N^{eq}(\vec{p})d\vec{p} = \int_{t_{eq}}^{\infty} dt \sum_n \lambda_j^i(n,E,T)P(E,n,t)\frac{\partial(p,\Omega)}{\partial(T,\Omega)}F(\Omega)dTd\Omega \ , \qquad (40)$$

where the time moment $t \to \infty$ corresponds to the complete deexcitation of a nucleus due to particle emission. As the nuclear states with different n are equally probable in the statistical equilibrium, the right-hand side of (40) is simplified to

$$\begin{aligned} N^{eq}(\vec{p})d\vec{p} &= \sum_n \lambda_j^i(n,E,T)P(E,n,t)\frac{\omega(n-1,E-B_j-T)}{\sum_{n'}\omega(n',E)}\frac{\partial(p,\Omega)}{\partial(T,\Omega)}F(\Omega)dTd\Omega \sim \\ &\sim T^{3/2}\sigma_{inv}(T)\frac{\sum_n \omega(n-1,E-B_j-T)}{\sum_{n'}\omega(n',E)}dTd\Omega \ . \end{aligned} \qquad (41)$$

By summing over n the total density of exited states $\omega(E) = \sum_n \omega(n,E)$ is reduced to an exponential form $\omega(E) \sim exp2\sqrt{gE}$. Thus, for $t \geq t_{eq}$ (or $n \geq n_{eq}$) we can use the conventional "evaporative" approximation by substituting in (34) $\omega(p,h,E) \to \omega(E) \sim exp2\sqrt{aE}$ with the level density a.

An important point of the CEM is the condition for transition from the intranuclear cascade stage to the pre-equilibrium processes. In the conventional cascade-evaporation models fast particles are traced down to some minimal energy, the cutoff energy T_{cut} being about 7-10 MeV below which particles are considered to be absorbed by the nucleus. The CEM uses another criterion according to which a primary particle is considered as part of the cascade, namely the proximity of the imaginary part of the optical potential $W_{opt.mod}(r)$ calculated in the cascade model to the experimental one $W_{opt.exp.}(r)$. This value is characterized by the parameter

$$\mathcal{P} = | \ (W_{opt.mod.} - W_{opt.exp.})/W_{opt.exp.} \ | \ . \qquad (42)$$

Here we use the fixed value $\mathcal{P} = 0.3$ extracted from the analysis [1]-[4] of experimental proton- and pion-nucleus data at low and intermediate energies.

One should note that in the CEM the initial configuration for the pre-equilibrium decay (number of excited particles and holes, i.e., excitons $n_0 = p_0 + h_0$, excitation energy E_0^* and linear momentum $\mathbf{P_0}$ of the nucleus) differs significantly from that usually postulated in exciton models. Our calculations [1]-[4] show that the distributions of residual nuclei remaining after the cascade stage of the reaction, i.e., before the pre-equilibrium emission, with respect to n_0, p_0, h_0, E_0^* and $\mathbf{P_0}$ are rather broad.

Complex particles can be produced in intermediate-energy nuclear reactions at different interaction stages and due to many mechanisms. These may include fast processes like direct knock-out, pick-up reactions or final state interactions resulting in coalescence of nucleons into a complex particle. The present version of the CEM neglects all these processes at the cascade interaction stage. Therefore, fast complex particles can appear in our model only due to pre-equilibrium processes. We assume that in the course of the reaction p_j excited particles are able to condense with probability γ_j forming a complex particle which can be emitted during the pre-equilibrium state. The "condensation" probability γ_j is estimated as the integral of overlapping the wave function of independent nucleons with that of the complex particle (cluster). Of course, slow complex particles may be evaporated along with nucleons at the compound stage of the reaction. We include the emission of n, p, d, t, ^{3}He and ^{4}He at both the pre-equilibrium and the evaporative stages of reaction. Pions in our CEM arise only from the processes (29) and leave the nucleus either directly or after additional rescatterings during the cascade.

The CEM predicts forward peaked in the laboratory system angular distributions for secondary particles. Firstly, this is due to high asymmetry of the cascade component (for ejected nucleons and pions). A possibility for forward peaked distributions of nucleons and composite particles emitted during the pre-equilibrium interaction stage is related to retention of some memory of the projectile's direction. In addition to energy conservation we need to take into account conservation of linear momentum $\mathbf{P}$ at each step as a nuclear state evolves. In a phenomenological approach this can be realized in different ways[1]. The simplest way used here consists in sharing the momentum $\mathbf{P_0}$ (similarly to energy E_0^*) between an ever increasing number of excitons involved in the interaction in the course of equilibration of the nuclear system. In other words, the momentum $\mathbf{P_0}$ should be attributed only to n excitons rather than to all A nucleons. Then, particle emission will be symmetric in the proper n-exciton system but some forward peaking will arise in both the laboratory and center-of-mass reference frame.

Recently, the CEM was developed by including the competition between particle emission and fission at the evaporative stages of reactions[26] and by including a more realistic nuclear level density with Z, N, and E^* dependences of the level density parameter[27]. At present, we develop the CEM for the description of the processes of γ-emission at all three stages of a reaction[28] in order to evaluate the relative role of different photon production mechanisms from proton-nucleus reactions at intermediate energies, and extend the CEM for the description of antinucleon-nucleus interactions.

In our calculations, all the CEM parameter values are fixed and are the same as in Ref.[1].

4. Exemplary Results and Discussion

We analyzed a large variety of data from nucleon-, pion-, and γ−induced reactions using the CEM (see Refs.[1]−[5], [26]-[29] and references given therein). A detailed comparison of the CEM predictions with the results of other current models may be found in the recent review[30]. Therefore, we confine ourselves to the discussion of some exemplary results. Measured[31] and calculated inclusive spectra of protons are shown in Fig. 2. The CEM reproduces well the change in the spectrum shape with increasing emission angle and in passing from light to heavy target-nuclei, providing correct absolute values for the particle yield for all incident energies.

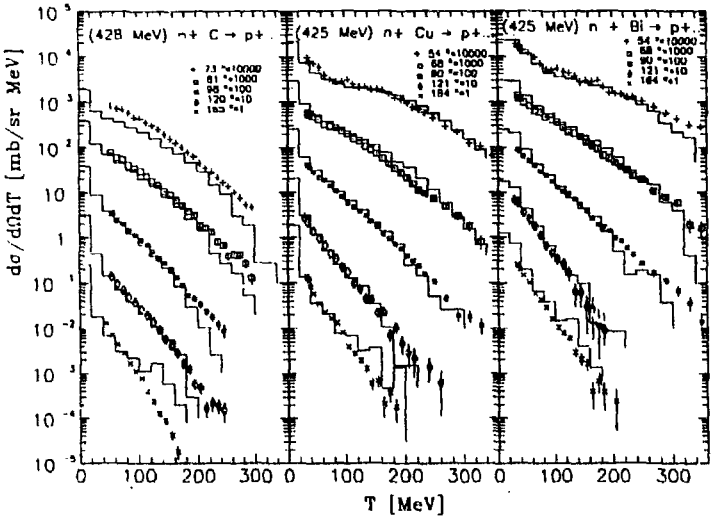

Fig. 2. Measured [31] inclusive proton spectra (symbols) and CEM calculations (histograms). Different emission angles (upper row) and different incident energies (lower row) are drawn with symbols as indicated. The histograms are the sum of all three CEM (cascade, pre-equilibrium and evaporative) components.

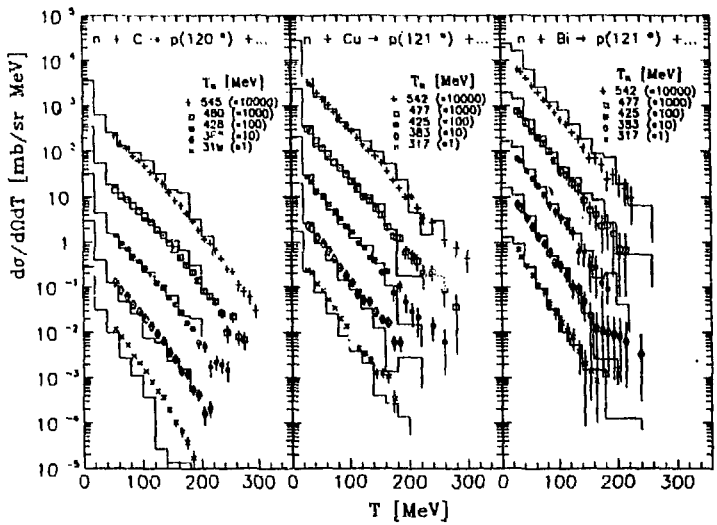

To illustrate the relative role of different proton production mechanisms for neutron-copper collisions at 425 MeV, as an example, the cascade, pre-equilibrium and the evaporative components of proton spectra are shown separately in the upper part of Fig. 3. One can see that the main contribution of slow protons to the spectra comes from the evaporation from compound nuclei, while with increasing ejectile energy the emission at the cascade and pre-equilibrium stages becomes dominant. The cascade component describes almost the entire measured spectra at forward angles, but with increasing angle of detection the relative role of the pre-equilibrium component rises considerably, and for very backward angles and proton energies less than 80 MeV the contribution of pre-equilibrium emission becomes comparable with that from the cascade.

For many applications and scientific problems it is necessary to analyze and evaluate not only data on nucleon production but also other characteristics as data on complex particle and pion production, fission cross sections. Some exemplary results are shown in Figs. 4 - 6.

Fig. 4 shows inclusive spectra of deuterons measured[31] and calculated with the CEM. The low energy parts of the complex particle spectra calculated in the CEM are formed by

particles evaporated at the compound stage of the reaction, while the high energy ones are

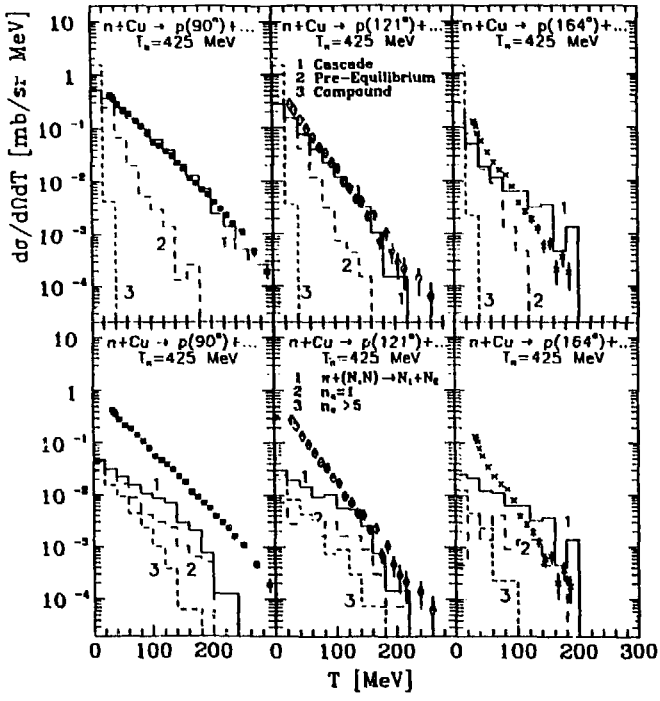

Fig. 3. Inclusive proton spectra from the neutron-copper collisions at 425 MeV. **Upper row:** the histograms 1, 2, and 3 show the contribution of cascade, pre-equilibrium, and evaporative components, respectively; **lower row:** for cascade component the histograms 1, 2, and 3 show the contribution from events which contain a two-step process of pion production in collisions of incident or cascade particles with nuclear nucleons (29) followed by pion absorption on nucleon pairs within this target-nucleus (30) in the course of the reaction (including all possible former and/or subsequent intranuclear collisions), the contribution from the events with $n_c = 1$, and $n_c > 5$, respectively. The value n_c is the number of successive interaction acts before proton emission in the events contributing to the corresponding histograms. The experimental points are taken from Ref. [31].

determined by the pre-equilibrium emission. It can be seen that the CEM reproduces correctly the shape and absolute value of the backward complex particle spectra. For forward angles the CEM significantly underestimates the experimental data (see, Ref.[3]). This happens because we neglect in our approach fast processes of complex particle production such as pick-up, knock-out and coalescence of complex particles from fast nucleons emitted during the cascade stage. Such processes contribute especially to the forward complex particle emission and their disregard in the CEM results in underestimation of complex particle spectra at forward angles. To describe better the complex particle spectra at intermediate energies the CEM must be improved by incorporating fast processes of complex particle production.

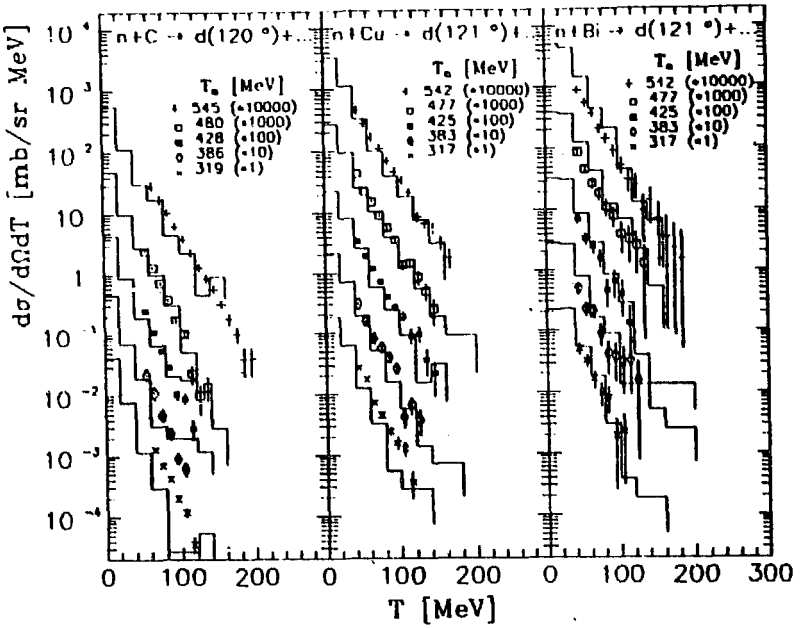

Fig. 4. Inclusive deuteron spectra: histograms are the sum of pre-equilibrium and evaporative components calculated within the CEM, the rest notation is the same as in Fig. 2.

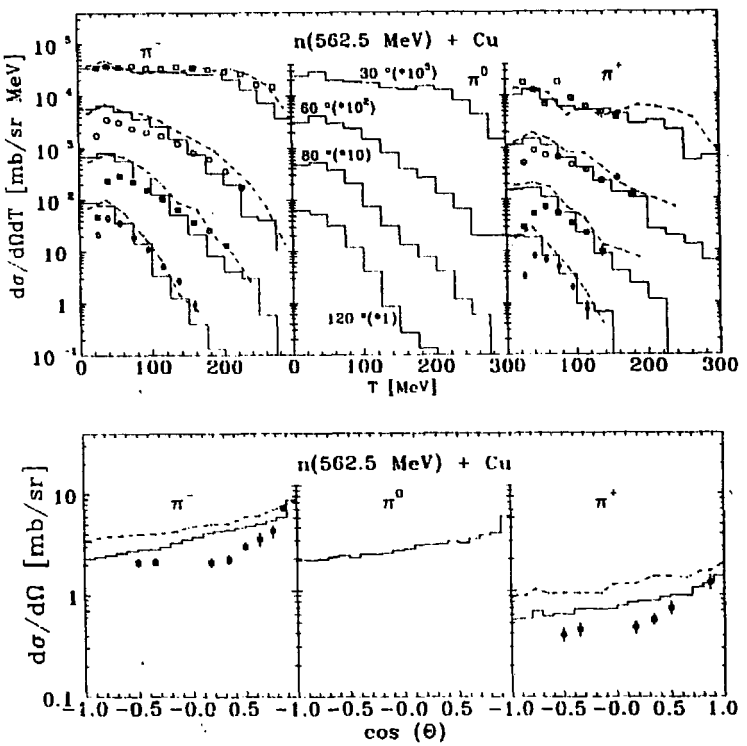

Fig. 5. Double differential cross sections at angles 30°, 60°, 80°, and 120° (upper row) and angular distributions for pion energies greater than 32.2 MeV (lower row) of three pion charge states for 562.5 MeV neutrons on Cu. The points are experimental data [32], the histograms and dashed lines are our CEM and LAHET [33] calculations from Ref. [32], respectively.

We have applied the CEM to analyze practically all known data on nucleon-induced pion production for intermediate and heavy nuclei and bombarding energies less than several GeV.

As an example, Fig. 5 shows part of the recent data[32] on neutron-induced inclusive π^- and π^+ production along with our CEM and LAHET [33] calculations from Ref.[32]. For comparison, spectra of neutral pions predicted by the CEM are also shown in the figure. One can see that both the CEM and Bertini's ICM give results in reasonable agreement with the data. Similar agreement was obtained for other reactions.

Recently, the CEM has been applied to analyze nucleon-, pion-, and photon-induced fission. As an example, the incident energy dependences of experimental and calculated with the CEM fission cross-sections for proton-gold and -uranium interactions are shown in Fig. 6. Analogous results have been obtained for other reactions.

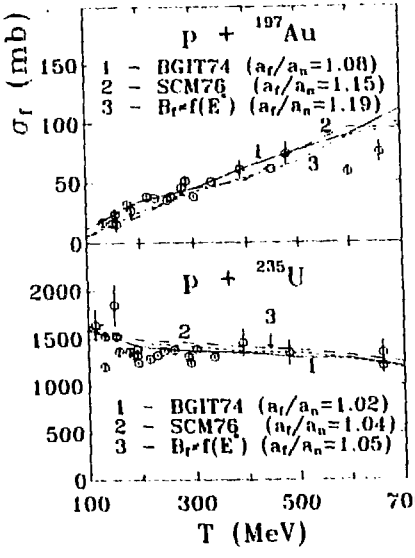

Fig. 6. Incident energy dependence of fission cross-sections for proton-gold and proton-uranium interactions. The experimental points are from the summary Table 159 of the monograph [21]. The lines are our CEM calculations performed with different fission barriers (for details see Ref. [26]) for the values of a_f/a_n shown in the figure.

Pion-nucleus interactions occupy a special place in intermediate energy nuclear physics due to touching upon different fundamental problems of nuclear reactions, hadron interactions and nuclear structure (see, the last reviews[34, 35]). One of the important modes of the pion-nucleus interaction is pion absorption (no pions in the final state). The cross section of this mode is large, in the Δ resonance region contributes about $\geq 1/3$ of the total pion-nucleus cross section; therefore, this mode affects significantly other pion-nucleus interaction modes.

Though good theoretical investigations have been performed in the last fifteen years and many interesting experimental results on pion absorption have been obtained at the meson factories in the USA, Canada and Switzerland, and at JINR, PNPI, KEK and CERN, an unambiguous interpretation of the observed phenomena has not been found yet[34, 35]. So, up to now there is no common point of view in literature on the questions: How many nucleons are involved in nuclear pion absorption? How does the reaction depend on the isospin of the absorbing system and on the energy of the pion?

Many measurements of pion-induced reactions have been performed especially with the purpose to obtain information on different pion absorption mechanisms (see reviews [34, 35]). So, McKeown et al. have measured inclusive (π, p) cross sections on ^{12}C, ^{27}Al, ^{58}Ni and ^{181}Ta at T_π = 100, 160 and 260 MeV [36]. Assuming that high-energy protons arise only from absorption reactions and neglecting the initial- and final-state interactions, McKeown et al. have analyzed their own data in a "hot spot" or a "slowly moving-source" representation and found that the number N_N of nucleons involved in the pion absorption is $N_N \sim 3$ for ^{12}C and increases to $N_N \sim 5.5$ for ^{181}Ta. This work had a large resonance in literature: afterwards

there were performed many theoretical investigations which demonstrated that McKeown's et al. data may be described by a 2N absorption mechanism, or on the contrary, only by multi-nucleon absorption (see reviews [34, 35]). Of great interest are also the recent measurements of pion-induced inclusive proton production on copper at 0.6, 0.8 and 1 Gev/c of Golubeva et al. [37]. By analyzing their own data and measurements by other authors in a "moving-source" representation, Golubeva et al. have found that the number of nucleons involved in pion absorption increases monotonically with pion energy from $N_N \sim 4$ at $T_\pi = 260$ MeV to $N_N \sim 18$ at $T_\pi = 4$ GeV.

We have analyzed, in our CEM, different characteristics of pion-nucleus interactions in the incident pion energy range up to ~3 GeV (see, e.g.,[2, 29, 35]). For our model there is no difference between nucleon- and pion-induced reactions. The first step of the cascade stage of the reaction is simply induced by a pion instead of a nucleon. Let us recall that in the CEM we regard only the 2N absorption mechanism (30).

As an example, a part of Golubeva's et al. data[37] are presented in Fig. 7 along with our CEM calculations and results of the best fit[37] in the moving-source model. For comparison, for proton spectra from 600 MeV/c π^+ interactions with Cu the results of the Dubna ICM calculation with the Δ isobar production in the intermediate states from Ref.[37] are shown in Fig. 7. One can see that both our CEM and the ICM equally satisfactorily describe the data only by the 2N absorption mechanism. (We obtained similar results for all other known data up to $T_\pi \sim 3$ GeV.) This indicates the importance of initial- and final- state interactions neglected by Golubeva et al. and McKeown et al. in analyzing their data by the "moving-source" representation.

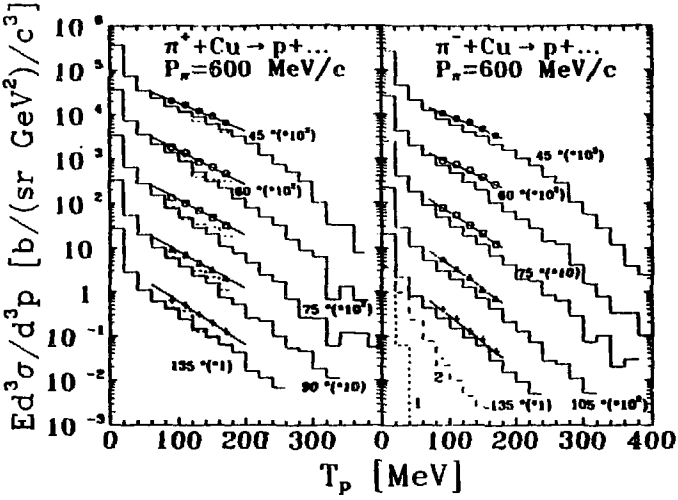

Fig. 7. Measured inclusive proton spectra from π^+ and π^- interactions with Cu at 600 MeV/c [37] (symbols), our CEM calculations (solid histograms), the results of the best fit in the moving-source model [37] (lines), and the calculations with the ICM with Δ as cascade participants from Ref. [37] (dashed histograms on the left graph). The dashed histograms 1 and 2 on the right graph show the CEM evaporative and pre-equilibrium components, respectively.

For spectra at 135°, the CEM pre-equilibrium and evaporative components are shown separately in Fig. 7. One can see that even at these relatively high incident energies the pre-equilibrium processes contribute to intermediate energy proton emission.

So, the CEM is able to describe data on pion-induced inclusive particle production in the absolute value without any free parameters (by taking into account only the 2N absorption mechanism (30)) and does not need to increase the mass of "clusters" absorbing pions with atomic mass of the targets or with incident pion energy. At the same time, one should note

that our model does not exclude some small contribution from pion absorption on heavier "clusters"[35].

The CEM has been developed [4] to describe also stopped negative pion absorption by intermediate and heavy nuclei. We again take into account only the 2N absorption mechanism. The point at which the pion is absorbed in the nucleus was determined from the distribution derived in [38] from calculations on pionic atoms $P_{abs} \sim exp[-(r-c)^2/2\sigma^2]$. The value of constants c and σ were determined by interpolating between the results given in [38] for nearby nuclei.

We have applied (see, e.g., Ref.[4, 39]) our model to analyze a large variety of experimental data on stopped negative pion absorption by nuclei from C to U: energy spectra and multiplicities of n, p, d, t, ^{3}He, and ^{4}He; angular correlations of two secondary particles; spectra of the energy released in the "live" ^{28}Si target on recording protons, deuterons and tritons in the energy range 40-70 MeV, 30-60 MeV and 30-50 MeV, respectively; isotope yields; nuclear fissilities; momentum and angular momentum distributions of residual nuclei, etc. As an example, Fig. 8 shows inclusive proton spectra measured recently by Gornov et al.[39], our calculation and the results reported by other authors (for details see [39]). On the whole, the CEM satisfactorily reproduces all the analyzed experimental data. This fact indicates that the 2N absorption mechanism is the main one for medium and heavy nuclei in the case of stopped pions as well. However, we have obtained [39] a direct indication on the α-particle absorption mechanism in ^{28}Si (on a level of $\sim$ 25%) from the analysis of spectra of energy released in the target for reactions with emission of tritons.

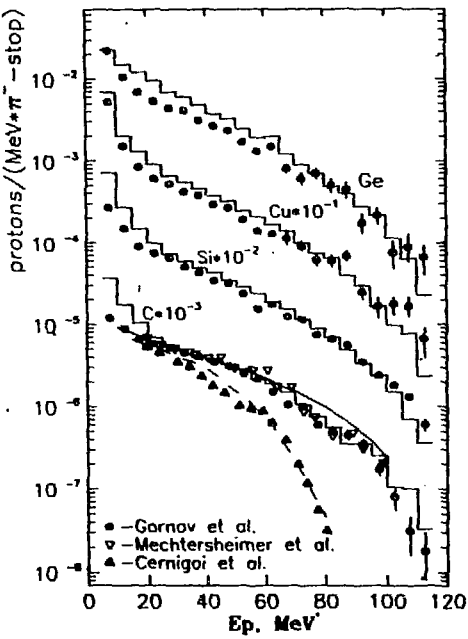

Fig. 8. Measured inclusive spectra of protons from reactions induced by stopped pions[39]−[41], our CEM calculations (histograms are the sum of all three CEM components), and the calculation based on the α-particle model[42], as indicated.

Recently, we extended the CEM to describe photonuclear disintegration at intermediate energies[5] using for the initial interaction of a photon with a nucleus the quasideuteron model in a manner similar to Ref.[43]. We analyzed photoabsorption cross sections; nucleon and pion spectra and multiplicities; neutron-proton coincidences; photofission cross sections and nuclear fissilities; excitation functions and isotope yields for reactions induced by photons with energies up to $\sim$ 1.2 GeV and target-nuclei from ^{12}C to ^{243}Am. As an example, in Fig. 9, the differential cross sections calculated within the CEM are compared with the data of Olson[44], and with the direct knockout[45], and quasideuteron[46] models for emergent protons at 43°, 90°, and 154° produced by 1.05-GeV bremsstrahlung on ^{12}C. One can see that a good agreement with experimental data in both the shape and absolute value has been obtained for protons emitted at both forward and backward angles.

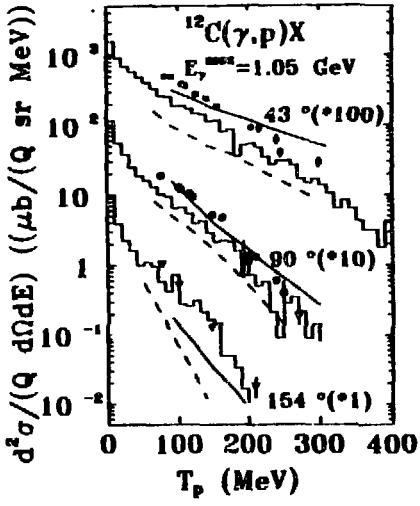

Fig. 9. Comparison of predicted inclusive proton spectra by the CEM (histograms are sums of all three CEM components) with $^{12}C(\gamma,p)X$ data of Ref.[44] (points), and with the direct knockout[45] (solid lines), and a quasideuteron model[46] (dashed lines).

Similar results were obtained for other reactions.

As it has been mentioned above, a most complete comparison of the CEM predictions with calculations in the framework of other current models may be found in the review[30] on the recent International Code and Model Intercomparison for Intermediate Energy Nuclear Reactions organized in 1992–1993 by the OECD Nuclear Energy Agency, Paris. The conditions of this Intercomparison were the following: There were a number of experimental data of interest, but unpublished, not available for participants. All the participants had to provide necessary calculations at their home Laboratories

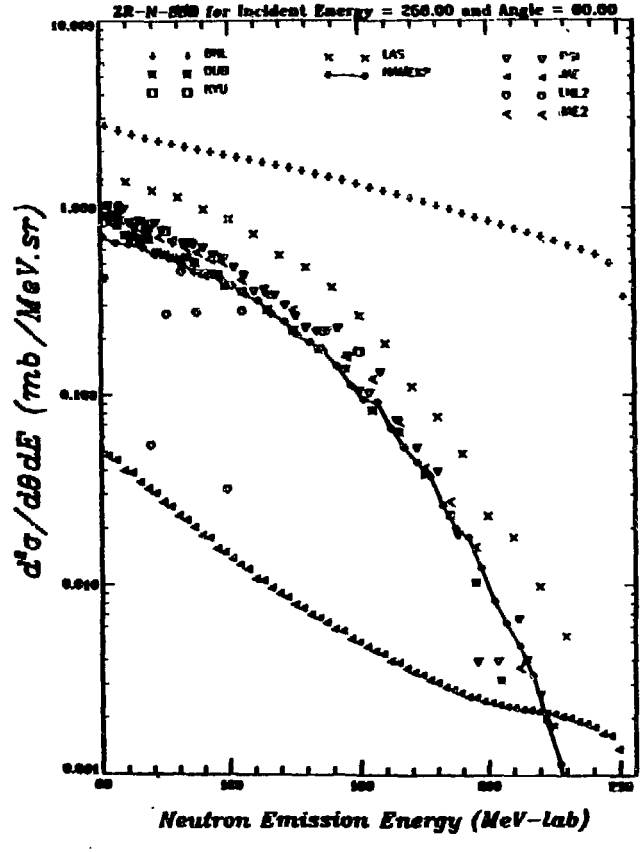

Fig. 10. Comparison of inclusive spectra of secondary neutrons from proton-zirconium collisions at 256 MeV predicted by several models with the experimental data[47] (solid line conecting symbols marked by HAMEEP), published when all the calculations were finished (for details see [30]). Symbols show the results obtained by different authors in the framework of different models, respectively: BNL - [48], DUB - our CEM calculations[49], KYU - [50], LAS - [51], PSI - [52], JAE - [53], LNL2 - [54], JAE2 - [55].

and then to send the results to the organizers at the NEA OECD. When all the calculations were finished the organizes compared the calculations with each other and with the unpublished experimental data. As an example, one typical figure from the review[30] is shown in Fig. 10. One can see that the CEM describes well nuclear reactions at intermediate energies and has one of the best predictive powers as compared to other available modern models. Other several hundreds of similar figures and tables may by found in Ref.[30].

5. Summary

Thus, we have shown how, using the Zubarev method of the non-equilibrium statistical operator, one may obtain the relativistic kinetic equations describing different stages of nuclear reactions in the CEM. For this, starting from a first principle, as the quantum relativistic Liouville equation, we had to use a series of anzatzes. The renounce of any concrete anzatz will arise the corresponding generalization of the kinetic equations used in the present version of the CEM and will improve our approach. We are working on this at present.

We have demonstrated that without any free parameters, the CEM is able to reproduce correctly shapes and absolute values of a large variety of nucleon- and pion-induced reaction data and can be applied to analyze the mechanisms of different nuclear reactions. The recent "International Code and Model Intercomparison for Intermediate Energy Reactions"[30] showed that the CEM adequately describes nuclear reactions at energies from 25 MeV to 1600 MeV and has one of the best predictive powers as compared to other available modern codes.

A recent modified version of our model allows one to calculate also photonuclear reaction data. A more recent modified version of the model is able to describe also emission of gamma rays. It is planned to make the recent versions of the code of the CEM available to users. They have an input simple and friendly for users and allow one to calculate different medium energy nuclear data in the absolute value without free parameters. A detailed description (User Manual) of the recent modified versions of the code is in preparation.

One may conclude that the Cascade-Exciton Model is indeed suitable for the evaluation of medium energy nuclear data for science and applications and for the analysis of different types of nuclear reactions. Further development and improvement of the CEM are possible, and a work in this direction is in progress at present.

We would like to thank Prof. G. Maino for inviting us to give our lectures and kind hospitality, as well as the whole staff of the Institute for Scientific Interchange Foundation for their efforts in maintaining a high standard of the meeting and very pleasant ambience at Villa Gualino, Torino, Italy. Last, but not least, we thank the European Science Foundation for financial support.

References

[1] K.K. Gudima, S.G. Mashnik and V.D. Toneev, Nucl. Phys. A401 (1983) 329; JINR Communications P2-80-774, P2-80-777, Dubna (1980)

[2] S.G. Mashnik and S. Tesch, Z. Phys. A312 (1983) 259; S.G. Mashnik, in: Proc. 18th Winter School Leningrad Inst. Nucl. Phys., vol. 3 (Leningrad, 1983) p. 172; S.G. Mashnik, S. Tesch and S.V. Dzemuhadze, Preprint Inst. Appl. Phys. 84-3, Kishinev (1984); V.N. Baturin et al., Preprint LINP-1302, Leningrad (1987); K.K. Gudima, S.G. Mashnik and

V.D. Toneev, JINR Communication E2-11307, Dubna (1978); V.I. Komarov et al., Nucl. Phys. **A326** (1979) 297

[3] S.G. Mashnik, Nucl. Phys. **A568** (1994) 703

[4] S. G. Mashnik, Revue Roum. Phys. **37** (1992) 179; Proc. 20th Winter School Leningrad Inst. Nucl. Phys., vol. 3 (Leningrad, 1985) p. 236; Preprint ICTP, Miramare-Trieste IC/92/39 (1992)

[5] T. Gabriel, G. Maino and S.G. Mashnik, "Analysis of Intermediate Energy Photonuclear Reactions", Proc. XII Int. Sem. on High Energy Phys. Problems "Relativistic Nuclear Physics & Quantum Chromodynamics", Dubna, Russia, September 12-17, 1994

[6] W. Cassing and U. Mosel, Proc. Part. Nucl. Phys. **25** (1990) 235

[7] S.-J. Wang, B.-A. Li, W. Bauer and J. Randrup, Ann. of Phys. **209** (1991) 251

[8] W. Botermans and R. Malfliet, Phys. Let. **B215** (1988) 617

[9] S. Mrowczynski and U. Heinz, Ann. of Phys. in press

[10] J.E. Davis and R.J. Perry, Phys. Rev. **C43** (1991) 1893

[11] W. Botermans and R. Malfliet, Phys. Rep. **198** (1990) 115

[12] Q. Li, J.Q. Wu and C.M. Ko Phys. Rev. **C39** (1989) 849

[13] A.V. Prozorkevich, S.A. Smolyansky and V.D. Toneev, Journ. of Theor. and Math. Phys. **95** (1993) 74; Preprint GSI-93-26 (1993)

[14] A.V. Prozorkevich, S.A. Smolyansky and V.D. Toneev, Proc. Int. Conf. "Meson and Nuclei at Intermediate Energies", Dubna, Russia, May 3-7, 1994

[15] A.V. Prozorkevich, S.A. Smolyansky and V.D. Toneev, Proc. XII Int. Sem. on High Energy Phys. Problems "Relativistic Nuclear Physics & Quantum Chromodynamics", Dubna, Russia, September 12-17, 1994

[16] C.M. Ko, Q. Li and R. Wang, Phys. Rev. Lett. **59** (1987) 1084

[17] H.-Th. Elze et al., Mod. Phys. Lett. **A2** (1987) 451

[18] Yu.B. Ivanov, Nucl. Phys. **A474** (1987) 669

[19] C.M. Ko and Q. Li, Phys. Rev. **C37** (1988) 2270

[20] X. Jin, Y. Zhuo, X. Zhang and M. Sano, Nucl. Phys. **A506** (1990) 655

[21] V.S. Barashenkov and V.D. Toneev, Interaction of High Energy Particles and Nuclei with Atomic Nuclei (Atomizdat, Moscow, 1972) in Russian

[22] K.K. Gudima, G.A. Ososkov and V.D. Toneev, Yad. Fiz. **21** (1975) 260; S.G. Mashnik and V.D. Toneev, Communication JINR P4-8417, Dubna (1974)

[23] T. Ericson, Adv. in Physics **9** (1960) 425

[24] F.C. Williams Jr., Phys. Lett. **B31** (1970) 180

[25] I. Ribanský, P. Obložinský and E. Běták, Nucl. Phys. **A205** (1973) 545

[26] S.G. Mashnik, Acta Phys. Slov. **43** (1993) 243

[27] S.G. Mashnik, Acta Phys. Slov. **43** (1993) 86

[28] S.G. Mashnik, Ye.S. Golubeva and A.S. Iljinov, Int. Conf. on Perspectives for the Interaction Boson Model on the Occasion of Its 20th Anniversary, Padova, Italy, June 13-17, 1994, Abstracts of Contributed Papers. p.39, and in progress

[29] S.G. Mashnik, Acta Phys. Pol. **B24** (1993) 1685

[30] M. Blann, H. Gruppelar, P. Nagel and J. Rodens, International Code Comparison for Intermediate Energy Nuclear Data (OECD, Paris, 1994)

[31] J. Franz et al., Nucl. Phys. **A510** (1990) 774

[32] M.L. Brooks et al., Phys. Rev. **C45** (1992) 2343

[33] H.W. Bertini, Phys. Rev. **188** (1969) 1711; R.E. Prael and H. Lichtenstein, Los Alamos National Laboratory version of the HETC Monte Carlo code which was originaly developed at Oak Ridge National Laboratory, LA-UR-89-3014, (1989)

[34] H.J. Weyer, Phys. Rep. **195** (1990) 295

[35] S.G. Mashnik, JINR Preprint E2-93-470, Dubna (1993); submitted to Yad. Fiz.

[36] R.D. McKeown et al., Phys. Rev. Lett. 44 (1980) 1033; Phys. Rev. **C24** (1981) 211

[37] M.B. Golubeva et al., Proc. 5th All-Union Sem. Program of Experimental Infestigations at the Meson Factory of the Inst. Yad. Isled. Akad. Nauk SSSR, Zvenigorod, April 12-15, 1987, (Moscow, Inst. Yad. Isled. Akad. Nauk SSSR, 1987), p.205, in Russian; Phys. Lett. **B221** (1989) 238

[38] A.S. Iljinov, M. Leon, R. Seki and S.E. Chigrinov, Preprint INR, Moscow, **P-0188** (1981)

[39] M.G. Gornov et al., Sov. J. Nucl. Phys., **47** (1988) 612

[40] G. Mechtersheimer et al., Nucl. Phys. **A324** (1979) 379

[41] C. Cernigoi et al., Nucl. Phys., **A456** (1986) 599

[42] D.F. Jackson and D.J. Berner, Prog. Part. Nucl. Phys., 5 (1981) 143

[43] V.S. Barashenkov et al., Nucl. Phys. **A231** (1974) 462

[44] D.N. Olson, Ph.D. thesis, Cornell University, 1960

[45] D.H. Boal and R.M. Woloshin, Phys. Rev. **C23** (1981) 1206

[46] J.L. Mattews and W. Turchinetz, LNS Internal Report No. 110., 1966

[47] S. Stamer et. al., Phys. Rev., **C47** (1993) 1647

[48] S. Pearlstein, BNL, USA: SYSTEMATICS, for details, see [11]

[49] S.G. Mashnik, JINR, Dubna, Russia: CEM, Ref. [1]; Fission, Ref. [26]; Levell Densities, Ref. [27]

[50] K. Ishibashi, H. Takada, N. Yoshizawa and Y. Nakahara, Kyushu University, Japan: Y.Nakahara and T. Nishida, JAERI-M86-074 (1986); K. Ishibashi, Proc. 12th Int. Coll. on Advanced Neutron Sources (ICANS XII), May 1993, Abingdon, UK; F. Atchinson, RL-81-006 (1981); K.C. Chandler and T.W. Armstrong, ORNL-4744 (1972); P. Cloth et al., KFA-IRE-E AN/12/88, 1988

[51] R.E. Prael, LANL, USA: R.E. Prael and H. Lichtenstein, LA-UR-89-3414, LANL (September 1989)

[52] F. Atchinson and H.U. Wenger, PSI, Switzerland: MECC, H.W. Bertini, Phys. Rev., **188** (1969) 1711; EVAP, L.W., Dresner ORNL-TM-196 (1962); Fission, F. Atchinson papaer II, Juel. Conf. **34** (1980) 17

[53] T. Fukahori, JAERI, Tokai-mura, Ibaraki, Japan: T. Fukahori, JAERI-M 92-039 (1992) 114; S. Pearlstein, J. Astrophys., **346** (1989) 1049

[54] G. Peilert, Inst. of Theor. Phys., Frankfurt, Germany: G. Peilert et al., Phys. Rev., C46 (1992) 1457

[55] H. Takada, T.Nishida and Y. Nakahara, JAERI, Tokyo, Japan: Y. Nakahara and T. Tsutsui, JAERI-M82-198 (1982); T. Nishida, Y. Nakahara and T. Tsutsui, JAERI-M-86-116 (1986); T. Nishida, Y. Nakahara and T. Tsutsui, JAERI-M87-088 (1987)

Received by Publishing Department
on September 2, 1994.